Investigation of large-scale pressure propagation and monitoring for CO_2 injection using a real site model

KATHARINA BENISCH & SEBASTIAN BAUER
Institute for Geosciences, University of Kiel, Ludewig-Meyn-Str. 10, D-24118 Kiel, Germany
kb@gpi.uni-kiel.de

Abstract This paper presents a study on monitoring of large-scale pressure evolution during and after CO_2 injection on a real site-scale model in the North German Basin. The study is aimed at identifying suitable locations for monitoring and at determining the conditions under which meaningful pressure signals can be measured. A multi-layered reservoir model is used, which contains two potential storage formations separated by a cap rock complex. CO_2 is injected into the lower storage formation. The pressure is monitored in several geological layers at varying distances from the injection well. Simulation results show that pressure increases both in the cap rock and below the storage formation. The pressure increase in the upper storage formation is only faintly detectable, so that no interaction between the two storage formations has to be expected. The type of boundary conditions used yield changes in the pressure signal at larger distances from the injection well, but not close to it. These results show that pressure monitoring and assessment is sensitive to individual site conditions and site geology, and has to be evaluated for each CCS project individually.

Key words CO_2 injection; monitoring; pressure propagation

INTRODUCTION

Monitoring of reservoir pressure is of significant importance for examining the storage process when CO_2 is injected into the subsurface. A detectable pressure signal can help to evaluate the radius of regional pressure influence and the pressure increase within the storage formation. This is important for assessing the storage capacity, since high injection pressures and a large-scale pressure increase lead to a lower injectable amount of CO_2 (Zhou *et al*., 2008). Rock and fluid properties, as well as reservoir boundary conditions, affect the height of the pressure increase. Most studies published so far have concentrated on the pressure increase in the injection formation, assuming impermeable over- and underlying formations. However, in a multi-layered reservoir, underlying and overlying formations are also affected by the pressure changes through their compressibility and permeability. This might result in a higher overall storage capacity, but may also effect neighbouring storage formations (Schäfer *et al*., 2011). Hence, assessing pressure increase and monitoring should be done in the lateral, as well as the vertical direction.

Vertical pressure build up has been investigated e.g. by Birkholzer *et al*. (2009) using strongly simplifying assumptions on the geological structure. In reality, geological formations are heterogeneous in a horizontal as well as in a vertical direction, and may show a complex vertical structure. Therefore, a profound study on the regional pressure signal resulting from different model conditions (e.g. multi layered, boundary conditions) for a real site geometry with non-horizontal layering is conducted. Using a real geological structure (including formations underlying and overlying the storage formation with different parameterizations) for the evaluation of pressure propagation and pressure monitoring provides a realistic setting for the ongoing processes and their scales. This study therefore investigates the effects of the vertical geological structure and of the large-scale setting on the pressure propagation. The results are used to determine suitable monitoring locations and to interpret the measured pressure signals.

MODEL SETUP

An anticline structure within the North German Basin is used for the CO_2 injection simulation. The model has a lateral extent of 29 × 28 km and an average vertical thickness of 2280 m. Figure 1 illustrates the geometrical shape of the multi-layered model. It represents a typical sedimentary deposition system with alternating permeable and impermeable strata.

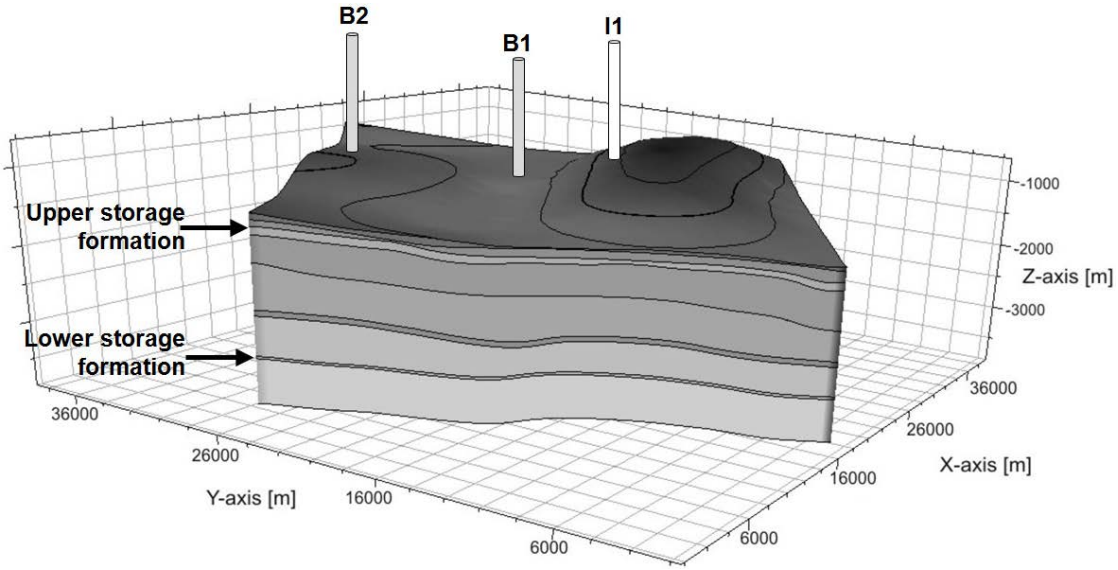

Fig. 1 Geological model (five times vertically exaggerated) based on information from borehole measurements and seismic data (Hese, 2009). The two potential storage formations as well as the injection (I1) and monitoring wells (B1 and B2) are marked.

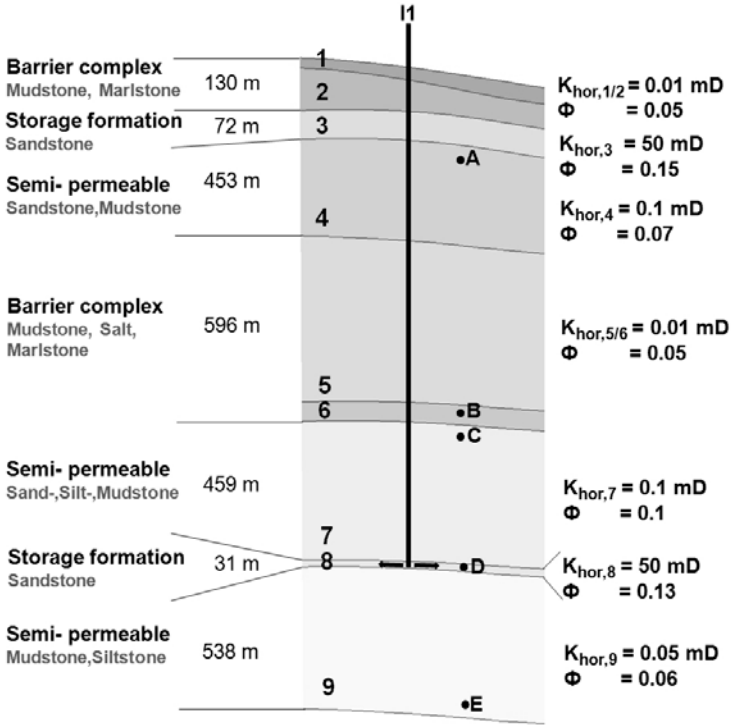

Fig. 2 Vertical profile of the geological model showing the reservoir stratigraphy and parameters. Formations 3 and 8 form the potential storage formations. Formations 1, 2, 5 and 6 are almost impermeable and can be assumed to act as possible barrier complexes. Points A, B, C, D and E mark the depths of pressure monitoring at wells B1 and B2. Porosity Φ and permeability K are indicated on the right side. The ratio K_{hor}/K_{ver} is 10.

The entire stratigraphy with overall nine different formations, as well as permeability and porosity values are shown in Fig. 2. The parameterization is based on borehole data and literature (Hese, 2009).

The geological model has an overall pore space volume of 1.4615×10^{11} m^3. It contains two formations, which may be suitable for CO_2 storage. Formation 8 is used as injection formation, as it consists mainly of fine sandstone, has an average thickness of 31 m and is located at an average depth of about 2815 m. It is overlain by a voluminous, semi-permeable formation (formation 7) consisting of an alternating sandstone-shale-stratigraphy. The next formations above (formation 5 and 6, see Fig. 2) form the main barrier complex. Shales, as well as several salt layers are dominant over this complex and some marl stones are embedded in the upper part. Below the injection formation extends a low permeability formation of shale and fine sandstone. Because of the irregular order of the aquifer–aquitard stratigraphy with varying formation thicknesses and an uneven topography, the pressure response due to CO_2 injection will propagate unevenly in vertical and horizontal directions.

Permeability and porosity of each formation are homogeneously distributed (values see Fig. 2). Three different property zones are defined for the model to differentiate the high permeable (Zone 1 including formations 3 and 8), semi-permeable (Zone 2 including formations 4 and 7) and low permeable (Zone 3 including formations 1, 2, 5, 6 and 9) formations. Values are listed in Table 1.

Table 1 Hydrologic parameters for the three defined material zones in the model.

	Rock compressibility [bar^{-1}]	Entry pressure [bar]	S_{res} Brine [-]	S_{res} CO_2 [-]
Zone 1	4.00×10^{-5}	0.5	0.38	0.00
Zone 2	4.50×10^{-5}	1.0	0.50	0.00
Zone 3	4.75×10^{-5}	5.0	0.60	0.00

For the injection formation (Zone 1), we chose a k_r–S_w curve measured by Bennion & Bachu (2006) for the Cardium Sandstone, which is relatively similar to the sandstone of formation 8. The Brooks-Corey k_r–S_w-relationship is used to define the curves for zones 2 and 3.

For the fluid phases, pressure dependency of compressibility, density and viscosity is accounted for in PVT tables. As CO_2 dissolution in brine is included in the simulations, changes in brine density occur.

The geological model is discretized into $65 \times 111 \times 23$ cells with a finer discretization around the injection well and within the injection horizon. The upper and lower model boundaries are closed. The lateral boundaries are set to constant hydrostatic pressure to enable pressure compensation by brine outflow across the boundaries. The boundaries are not completely open, but are subject to a specific storage volume, which was estimated from the real large-scale geological conditions around the model area. Initially, hydrostatic pressure is set within the model as well as a constant salinity of 5000 mg/L. Temperature is constant at 84°C. CO_2 is injected into formation 8 through one well I1 (location see Fig. 1) with a rate of 1 million tons per year for 20 years. After injection ceases, 60 years of the post-injection period are simulated to investigate the longer term pressure evolution.

SIMULATION RESULTS

Base scenario

For the investigation of the large-scale pressure behaviour over time, the pressure change at five different depths (see Fig. 2) and several distances from the injection well are depicted in Fig. 3. At the injection well at depth D (Fig. 3(a)), the pressure signal is mainly influenced by the injection pressure. The maximum pressure change adds up to 180 bars at the beginning of the injection,

which corresponds to an increase of 64% of the initial hydrostatic pressure. As this study is focused on the large-scale effects of a CO_2 injection, no efforts were undertaken to dampen the high injection pressure. Rather, it is assumed, that for a real site the injection would be spatially distributed in order not to reach the fracture closure pressure. With higher saturation of CO_2, the pressure decreases slightly during injection since the relative permeability for CO_2 increases. After 20 years, the injection stops and a pressure drop can be observed, with pressure decreasing towards the initial pressure within the next decades.

For the other depths at the injection well, pressure signals become smaller with increasing vertical distance from the injection formation and decreasing permeability of the respective layer (see Fig. 3(a)). At depth C, a maximum pressure change of 60 bars is still measurable. Because of the low permeability of formations 5 and 9 and a larger distance to formation 8, the pressure signals at depth B and E are slightly delayed and only half of the pressure signal at depth C. Also, the time curve is much smoother. Pressure tends towards the initial values at all monitoring depths, as the pressure increase can be compensated by flow across the model boundaries. There is only a very small pressure signal observed at depth A, showing that the thick low permeable formations 6 and 5 act as an effective barrier.

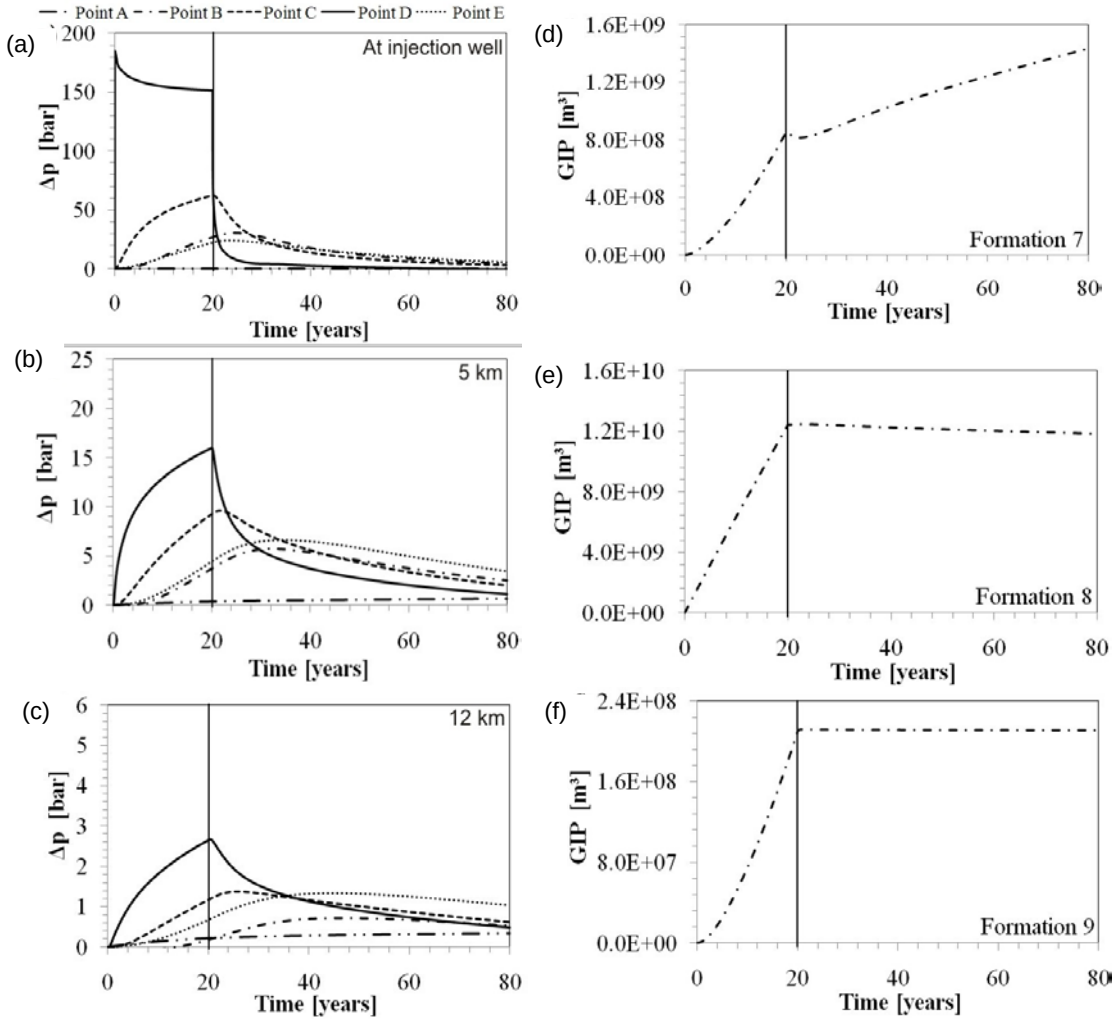

Fig. 3 Left side: Time evolution of pressure change at (a) injection location, (b) 5 km distance and (c) 12 km distance at depth A, B, C, D and E. Right side: Cumulative CO_2 in place (GIP) for (d) formation 7, (e) formation 8 and (f) formation 9. Note the different scales of the ordinate. The black vertical line marks the end of the injection.

Figure 3(b) and (c) show the large-scale pressure evolution at 5 and 12 km distance from the injection well. Generally, the pressure increase is smaller for larger distances from the injection well for all depths. The strongest pressure signal can be observed in the injection formation, where the maximum of the pressure increase is reached at the end of the injection. For all other locations, pressure increase is smaller, but the maximum is reached up to 20 years after injection stops and pressure only slowly returns to its initial level after that. This time lag increases with increasing distance and demonstrates the time frame required to return to the initial state.

In a multi-layered model with semi-permeable formations, the injected CO_2 will not only remain in the injection formation. Figure 3(d)–(f) show the time evolution of total CO_2 in the geological formations (GIP) for formations 7, 8 and 9. A total volume of 1.35×10^{10} m^3 of CO_2 was injected in formation 8, of which 87% remains there after 80 years. 10% of the CO_2 has spread upwards into the semi-permeable formation 7 (see Fig. 3(d)). Influx is high during the injection period, mainly induced by the pressure gradient. Density driven flow causes further accumulation of CO_2 in formation 7 as CO_2 rises from the injection formation. Figure 3(f) shows that about 3% of the injected CO_2 has flowed downwards during the injection period. There is only a low decrease in GIP after the injection stops, because the low permeability of formation 9 impedes the density driven rise back into formation 8. In comparison, the vertical permeability of formation 7 and therefore the upward flow of CO_2 after injection stops are much higher.

Boundary conditions

A precise investigation of the geological boundaries surrounding the model area is necessary to predict the pressure build up, as the boundaries may allow for brine discharge out of the formation and thus pressure relief. For the base scenario, the real storage volume of $1.4771 \cdot \times 10^{12}$ m^3 surrounding the injection formation was calculated and used. The boundary volume is thus 10 times larger than the model pore volume. The following evaluation addresses the effects of different boundary conditions on pressure build up.

Table 2 lists the simulated scenarios with their respective boundary conditions. Besides completely open and closed boundaries, we also consider different fractions of the real storage volume around the model area to analyse the transition from open to closed boundary conditions.

Table 2 Sensitivity of boundary conditions; list of the simulated scenarios.

Scenario no.	Boundary type	Real boundary storage %
0 (Base scenario)	Open (constant head)	100
1	Open (constant head)	Infinite
2	Open (constant head)	10
3	Open (constant head)	1
4	Open (constant head)	0.1
5	Open (constant head)	0.01
6	Closed	0

Figure 4 shows the pressure evolution at depth B and D at 12 km distance, where the influence of the boundary conditions is most apparent. Close to the injection well, the change in boundary conditions only has a small influence on the pressure build up.

Compared to the base scenario, there are no differences between infinitely open boundaries, the real storage volume and a storage volume of 10% and 1% of the real volume (scenarios 0–3). In all scenarios, pressure decreases towards the initial value, which means that the pressure build up is compensated by brine flow across the boundaries. For scenarios 4 and 5, the boundary volume is small in comparison to the base scenario and the model area. As a result, a higher maximum signal and a slower decrease in pressure after injection stops are observed.

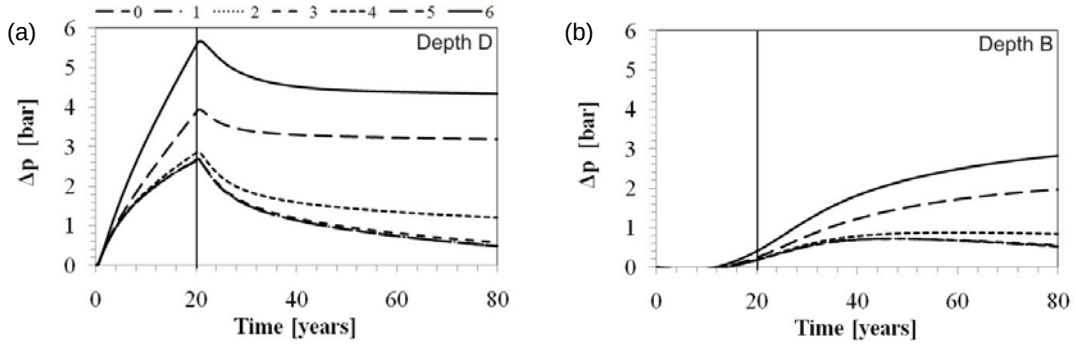

Fig. 4 Time evolution of pressure change for the scenarios listed in Table 2 at (a) depth D and (b) depth B 12 km from the injection well. The black vertical line marks the end of injection.

Also, pressure does not return to the initial value, as flow across the boundaries is restricted. The remaining pressure difference at the end of the simulation becomes higher with less boundary volume. The highest pressure increase can be seen for the closed boundaries. For long times, pressure will equilibrate and all depths will show the same pressure increase.

CONCLUSION AND OUTLOOK

Large-scale pressure build up due to injection has been investigated in the vertical as well as the lateral direction for a real site geometry to determine suitable locations for pressure monitoring. Generally, the strongest pressure signals are observed at the injection well for all monitoring depths. The injection start and stop becomes apparent in the time evolution of the pressure signals and a maximum pressure change of at least 20 bars occurs up to the cap rock. With increasing lateral distance, the maximum pressure signal gets smaller and pressure decreases more slowly after injection stops. Vertically, the pressure signal also decreases with distance and a delay in the pressure signal becomes obvious. Only in the injection formation, the pressure signal reflects the injection time without any delay. Above the cap rock, no meaningful pressure signal can be detected.

As the reliability of a monitoring strategy depends on the monitoring objective, different site locations may be suitable. The results show that monitoring locations between the injection formation and the cap rock at distances from the injection well up to 5 km are suitable for monitoring the injection process, as the time curve of the pressure signal reflects the injection operation. However, a delay in the pressure signal at larger distances from the injection well has to be taken into account. Locations far from the injection well are suitable for monitoring the large-scale pressure evolution and validating of boundary conditions, because they are sensitive to the large-scale setting. A location above the cap rock could be used to monitor the integrity of the cap rock. The time of highest leakage potential depends on the time lag of the pressure signal in the cap rock. As a consequence, further potential storage formations above the cap rock would not be available, if the formation is used for integrity monitoring.

Different boundary conditions lead to a change in time evolution and height of the pressure signal. For the used site geometry, the pressure signal behaves similarly for infinitely open boundaries as for the realistic storage volume. A stronger pressure signal is observed for closed or nearly closed boundary conditions. Therefore, reservoirs with closed boundaries show a higher pressure increase, but only if the monitoring well is in the same hydraulic compartment.

As can be seen from the results, the complex vertical structure of the model has a strong impact on the vertical pressure build up. The height and the time lag of the pressure signals observed at monitoring points far away from the injection well are influenced by the embedded formations. Thus the large scale pressure build up is strongly site specific and could not be represented correctly when using simplified models, which e.g. focus on the storage formation and do not include underlying and overlying formations.

In future work, more realistic injection scenarios with higher injection rates and multiple well configurations, heterogeneities and a more differentiated stratigraphy will be investigated. Furthermore, studies regarding the quantification of the time lag in the pressure signals at larger distances from the injection well will be performed.

REFERENCES

Bennion, B. & Bachu, S. (2006) Dependence on temperature, pressure, and salinity of the IFT and relative permeability displacement characteristics of CO_2 injected in deep saline aquifers. In: *SPE Annual Technical Conference and Exhibition*, Paper SPE 102138. (24–27 September, San Antonio, Texas, USA).

Birkholzer, J. T., Zhou, Q. & Tsang, C.-F. (2009) Large-scale impact of CO_2 storage in deep saline aquifers: A sensitivity study on pressure response in stratified systems. *Int. J. Greenhouse Gas Control* 3(2), 181–194.

Hese, F. (2009) Geologisches 3D Modell der Region Wagrien. LLUR S-H, Flintbek (unpublished report).

Schäfer, F., Walter, L., Class, H. & Müller, C. (2011) The pressure impact of CO_2 storage on neighbouring site, 10th International Conference on Greenhouse Gas Control Technologies. *Energy Procedia* 4, 4465–4471.

Zhou, Q., Birkholzer, J. T., Tsang, C.-F. & Rutqvist, J. (2008) A method for quick assessment of CO_2 storage capacity in closed and semi-closed saline formations. *Int. J. Greenhouse Gas Control* 2(4), 626–639.